European Review for Medical and Pharmacological Sciences 2022; 26: 5380-5392

In vitro mitochondrial apoptosis of melanoma cells *via* immature *Poncirus trifoliata* fruit extract

S.-Y. KIM[1], I.H. CHOI[2], M.J. HAN[2], H.-K. YI[3], B.-S. YUN[4], H.-R. PARK[5], M. KIM[1,2]

[1]Research Institute of Clinical Medicine of Jeonbuk National University – Biomedical Research Institute of Jeonbuk National University Hospital, Jeonju, Korea
[2]Department of Pediatrics, Jeonbuk National University Medical School, Jeonju, Korea
[3]Department of Oral Biochemistry, Institute of Oral Bioscience, School of Dentistry, Jeonbuk National University, Jeonju, Korea
[4]Division of Biotechnology and Advanced Institute of Environment and Bioscience, Jeonbuk National University, Iksan-si, Korea
[5]Department of Food Science and Biotechnology, Kyungnam University, Changwon-si, Korea

Abstract. – OBJECTIVE: ***Poncirus trifoliata (P. trifoliata)*** **fruits exert phytotherapeutic effects, depending on their maturity level. However, the mechanism by which these phytotherapeutic effects are exerted remains undefined – especially in cancers. Therefore, in this study, we investigated the effects of the immature fruit extract of *P. trifoliata* on a B16 melanoma cell line.**

MATERIALS AND METHODS: The effect of immature *P. trifoliata* extract on B16 cells was evaluated by MTT assay, cell proliferation, FACScan analysis of cell cycles, confocal imaging analysis, nuclear (Hoechst) staining, apoptosis assay (Annexin V-fluorescein isothiocyanate/propidium iodide staining), and Western blot assay. The capacity of immature *P. trifoliata* extract to inhibit the invasion and migration of B16 cells was assessed using the scratch-wound assay and Matrigel migration assay. The effect of immature *P. trifoliata* extract on mitochondrial function was determined *via* the mitochondrial membrane potential assay, activity, and fraction and cytosol proteins.

RESULTS: Treating B16 cells with a methanol extract of immature *P. trifoliata* (MEPT) significantly inhibited cell viability, migration, and invasiveness in a dose- ($p<0.01$) and time ($p<0.01$)-dependent manner. MEPT arrested the cells in the G1 phase of the cell cycle and led to the activation of the PI3K/AKT/p21 pathway. Furthermore, MEPT dose-dependently induced apoptosis in B16 cells by increasing the expression of the pro-apoptotic proteins Bax and Apaf-1, while decreasing the expression of the anti-apoptotic protein, Bcl-2. MEPT treatment also decreased mitochondrial membrane potential.

CONCLUSIONS: Immature *P. trifoliata* extract inhibited the growth of melanoma cells by inducing cell apoptosis through mitochondrial pathways. Therefore, further research into immature *P. trifoliata* extract as a potential therapeutic compound for melanoma treatment is warranted.

Key Words:
Immature *Poncirus trifoliata* fruit extract, Melanoma, Apoptosis, Mitochondria.

Introduction

Melanoma is the most fatal and aggressive type of skin cancer[1]. Melanoma accounts for about 1%-4% of all malignant skin tumors, but it results in 80% of skin cancer deaths. In cases of metastatic melanoma, the five-year survival rate of melanoma is only 14%[2,3]. The incidence of melanoma is higher in Caucasians (lighter skin) compared to individuals with low-risk phenotypes (darker skin), and this difference is due to the higher concentrations of photo-protectable epidermal melanin found in darker-skinned individuals[2]. In Caucasian populations, no difference in melanoma incidence and mortality exists between sexes[4]; moreover, once metastasis occurs, the prognosis remains very poor[5,6]. The primary treatment options for melanoma include surgical resection, chemotherapy, photodynamic therapy, immunotherapy, biochemotherapy, and targeted therapy. Adjuvant therapies, such as targeted therapy and immunotherapy, have been shown to increase survival rates of melanoma patients[5]. Surgery depends on the clinicopathological features of the tumor, while chemotherapy is considered in metastatic cases[1]. If metastatic or complete resection is not possible, the average survival rate of melanoma is less than a year[7]. These therapies, however, have some limitations: in addition to the skin and gastrointestinal toxicity induced

Corresponding Author: Minsun Kim, MD, Ph.D; e-mail: children@jbnu.ac.kr

by these therapies, resistance to immunotherapy, chemotherapy, and intralesional therapy (as well as to most other anticancer treatments) is common[1]. New therapeutic options based on a better understanding of the molecular pathogenesis of melanoma are thus needed.

The fruits of *Poncirus trifoliata* (L.) Raf. have been used as a traditional medicine in East Asian countries for various inflammatory diseases[8]. *P. trifoliata* is reported to exert different phytotherapeutic effects, depending on the maturity and active constituents of the fruits[9]. Mature fruits are known to have anticancer and anti-inflammatory properties, whereas immature fruits are known to influence gastrointestinal motility[9]. A recent study[10] has shown that immature fruits can be effective in cancer treatment. However, to our knowledge, no research has explored the anticancer effects of immature *P. trifoliata* fruit extracts on melanoma. Therefore, we evaluated the antitumor effect of immature *P. trifoliata* extract on B16 melanoma cells and established the underlying molecular mechanisms associated with this effect. This study provides valuable insights regarding the application of immature *P. trifoliata* fruit extracts in the development of anti-melanoma compounds.

Materials and Methods

Cell Line and Culture

A murine melanoma B16 cell line was purchased from the Korea Cell Line Bank (Seoul, Korea). The cells were maintained in Dulbecco's Modified Eagle Medium (DMEM; Gibco BRL Life Technologies, Gaithersburg, MD, USA), supplemented with 10% heat-inactivated fetal bovine serum (FBS), 300 μg/mL L-glutamine, 100 U/mL penicillin G, and 100 μg/mL streptomycin (all obtained from Gibco BRL Life Technologies, Gaithersburg, MD, USA). Cell cultures were incubated at 37°C in an atmosphere containing 95% air and 5% CO_2.

Preparation of Immature Fruit Extract of P. trifoliata

The isolation and purification of immature *P. trifoliata* (MEPT) methanol extract were performed as previously described[10]. Briefly, MEPT was obtained from the immature fruits of *P. trifoliata* by extraction with 70% aqueous methanol. The MEPT was subsequently concentrated under reduced pressure to obtain a residue that was then resuspended in distilled water. MEPT was then extracted with hexane and ethyl acetate. The ethyl acetate-soluble fraction was subjected to silica gel column chromatography (230-400 mesh, Ø 10 × 17 cm; Merck, Kenilworth, NJ, USA) using a stepwise solvent system of chloroform or methanol (from 100:1 to 20:1; volume/volume). The active fraction was re-chromatographed on a silica gel column (Ø 5 × 11 cm) and eluted with chloroform/methanol (50:1; volume/volume). Active fractions were sequentially chromatographed on a Sephadex LH-20 column (Ø 2.5 × 80 cm; GE Healthcare Bio-science AB, Uppsala, Sweden). The fractions were then eluted with 80% aqueous methanol on an ODS Sep-Pak C_{18} cartridge (10 g; Alltech Associates, Deerfield, IL, USA), to finally obtain MEPT as a glabretal triterpenes complex – partially purified by the isolation procedure.

Proliferation Assay

The effect of MEPT on cell viability was evaluated using the 3-(4,5-dimethylthiazol-2-yl)-2,5-diphenyltetrazolium bromide (MTT) assay. B16 cells were seeded in 96-well plates (1×10^4 cells/well) and incubated overnight. After treating the cells with MEPT at various concentrations (0, 10, 20, 30, and 40 μM; 10 μM = 0.0066 mg MEPT/mL)[10], at the appropriate time points (0, 24, 48, and 72 hours), 100 μL of MTT reagent was carefully added along the sides of each well. The cells were then incubated for 3-4 hours. The plates were then centrifuged and had dimethyl sulfoxide added to them. Absorbance at 540 nm was measured using a microplate reader (VersaMax ELISA microplate; Molecular Devices, San Jose, CA, USA).

In vitro Wound-Healing Assay

B16 cells were seeded in a 12-well plate (2×10^5 cells/well) and incubated overnight. Then, a sterile 20-200 μL pipette tip was held vertically to scratch a cross in each well, and the cells were treated with various concentrations (0, 10, 20, and 30 μM) of MEPT. After 0, 24, and 48 hours of incubation, the cells were photographed using an inverted microscope with 40× magnification (EVOS XL; Thermo Fisher Scientific, Waltham, MA, USA).

Matrigel Migration Assay

Transwell plates with Matrigel coating and pore size of 8 μm (Corning Inc., Corning, NY, USA) were used for the migration assay. A total of 5×10^4 cells, suspended in serum-free DMEM, were plated into the upper chamber of the Matrigel-coated transwell plates. MEPT at various concentrations (10, 20, and 30 μM) was plated in the

lower chamber, acting as a chemoattractant. The cells were incubated for 24 hours. Following incubation, non-migrated cells were removed using a cotton swab; migrated cells were fixed with 100% methanol for 15 minutes at 37°C and subsequently stained with Gram crystal violet (BD Biosciences, Heidelberg, Germany) for 10 minutes at 37°C. Cell numbers were counted in five separate fields and photographed using an inverted microscope with a 100× objective (EVOS XL; Thermo Fisher Scientific, Waltham, MA, USA).

FACScan Analysis of Cell Cycle

B16 cells were washed with phosphate-buffered saline (PBS) and fixed in cold 70% ethanol, on ice, for at least 30 minutes. The cells were washed again in PBS and stained with propidium iodide (PI, 6 μg/mL), at 4°C, for at least 30 minutes. Fluorescence intensities were measured using a FACScan flow cytometer (BD Biosciences, Foster City, CA, USA).

Mitochondrial Membrane Potential Assay

B16 cell mitochondrial membrane potential was assayed using a Muse™ MitoPotential Kit (Merck Millipore, Burlington, MA, USA), according to the manufacturer's instructions. Briefly, the cells were washed with PBS, and cell pellets were stained with the Muse™ MitoPotential Kit, for 25 minutes, at 37°C. Data were acquired using a Muse™ Cell Analyzer (Merck Millipore, Billerica, MA, USA). Calculations were performed automatically by the Muse Software Module (Merck Millipore, Billerica, MA, USA).

Mitochondrial Activity and Confocal Imaging Analysis

B16 cells were cultured on collagen-coated coverslips and incubated with MitoTracker Red CMXRos (100 nmol/L; Invitrogen, Carlsbad, CA, USA), for 30 minutes, according to the manufacturer's instructions. Next, the cells were counterstained with 4′,6-diamidino-2-phenylindole dihydrochloride (DAPI; Sigma-Aldrich, St. Louis, MO, USA) to localize merged images. Imaging analysis was performed using fluorescence microscopy (model LSM510; Carl Zeiss, Ostalbkreis, Germany).

Mitochondrial Fraction and Cytosol Proteins

A Mitochondria/Cytosol Fraction Kit (Biovision, Mountain View, CA, USA) was used for cellular fractionation. Briefly, B16 cells were washed with PBS and homogenized using a sonicator in an ice-cold cytosol extraction buffer mix containing dithiothreitol and a protease inhibitor. The homogenates were centrifuged at 700 ×g for 10 minutes at 4°C, and the supernatants were collected. The supernatants were then centrifuged at 10,000 ×g for 30 minutes at 4°C. The supernatant contained cytosol proteins, and the pellets were resuspended with ice-cold mitochondria extraction buffer (containing dithiothreitol and a protease inhibitor for mitochondrial proteins).

Nuclear (Hoechst) Staining

B16 cells were washed with PBS and fixed with 3.7% paraformaldehyde (Sigma-Aldrich, St. Louis, MO, USA), for 10 minutes, at 25°C. The fixed cells were washed with PBS, and 200 μL of Hoechst 33258 staining solution (Sigma-Aldrich, St. Louis, MO, USA) was added. The cells were then incubated for 30 minutes at 25°C. After incubation, the cells were directly observed using fluorescence microscopy (LSM510, 100× magnification; Carl Zeiss, Ostalbkreis, Germany).

Apoptosis Assay

An apoptosis assay was carried out using Annexin V staining (BD Pharmingen, BD Biosciences, San Jose, CA, USA), according to the manufacturer's protocol. The cells were washed with cold PBS and resuspended in 500 μL of the binding buffer (10 mM HEPES/NaOH pH 7.4, 140 mM NaCl, and 2.5 mM $CaCl_2$) at a concentration of 1×10^6 cells/mL. Annexin V-fluorescein isothiocyanate (FITC, 5 μL) and propidium iodide (PI, 1 μg/mL) were then added to the cells, and the cells were analyzed with a BD FACSCalibur™ (BD Biosciences, Foster City, CA, USA).

Protein Extraction and Western Blot Analysis

B16 cells were lysed on ice in a lysis buffer (containing 50 mM Tris-HCl, 150 mM NaCl, 1% Triton X-100, 1% sodium deoxycholate, 0.1% sodium dodecyl sulphate, and protease inhibitors). The protein concentration in cell lysates was measured using a protein quantification kit from Bio-Rad (Hercules, CA, USA). Twenty micrograms of protein per lane were loaded onto 8-15% sodium dodecyl sulfate-polyacrylamide gels (SDS-PAGE) and transferred to the polyvinylidene difluoride (PVDF) membrane. Non-specific antibody binding sites were blocked upon incubation with 5% skimmed milk in Tris-buffered saline with 0.1% polysorbate 20

(TBST-20). The membrane was then probed at 4°C, overnight, with primary antibodies, against the following proteins: phosphorylated phosphoinositide-3-kinase (p-PI3K, 1:1,000; #173665S), total phosphoinositide-3-kinase (PI3K, 1:1,000; #4249), phosphorylated-protein kinase B (p-AKT, 1:1,000; #9272), total AKT (1:1,000; #4051), cyclin E (1:1,000; #20808S), apoptotic protease activating factor-1 (Apaf-1 1:1,000; #8723S), cleaved caspase 3 (1:1,000; #9661), cleaved caspase 9 (1:1,000; #9501), poly (adenosine diphosphate-ribose) polymerase (PARP, 1:1,000; #9548; all from Cell Signalling Technology, Beverly, MA, USA); p21 (1:1,000; SC-6246), cytochrome c (1:1,000, SC-13156), B-cell lymphoma 2 (Bcl-2 1:1,000, SC-7382), Bax (1:1,000, SC-7480; all from Santa Cruz Biotechnology, Santa Cruz, CA, USA); and actin (1:2,000; A2066; Sigma-Aldrich, St. Louis, MO, USA). A horseradish peroxidase(HRP)-conjugated anti-rabbit IgG (#7074S) and an anti-mouse IgG (#7076S; both from Cell Signaling Technology, Danvers, MA, USA) were used as secondary antibodies, at a concentration of 1:3,000, for one hour at 25°C. Antibody-antigen binding was detected using Immobilon Western chemiluminescent HRP substrate (Millipore, Billerica, MA, USA). The images were acquired and analyzed using a chemiluminescence imaging system (Fusion Solo System; Vilber Lourmat, Paris, France).

Liquid Chromatography Mass Spectrometry (LC/MS) Analysis

Unbiased metabolomic analyses were performed using an ultra-performance liquid chromatography (UPLC) system (Waters, Milford, MA, USA). Chromatographic separation was carried out using an ACQUITY UPLC HSS T3 column (100 mm × 2.1 mm, 1.8 µm, Waters), with a column temperature of 40°C and a flow rate of 0.5 ml/min, where the mobile phase contained solvents A (water + 0.1% formic acid) and B (acetonitrile + 0.1% formic acid). Metabolites were eluted using the following gradient elution conditions: 97%, phase A, for 0-5 minutes; 3-100% linear-gradient, phase B, for 5-16 minutes; 100%, phase B, for 16-17 minutes; 100-3% reverse liner gradient, phase B, for 17-19 minutes; 97%, phase A, for 19-25 minutes. The loading volume of each sample was 5 µL. Metabolites eluted from the column were detected by a high-resolution tandem mass spectrometer, SYNAPT G2 Si HDMS QTOF (Waters), in positive and negative ion modes. For positive ion mode, the capillary and cone voltages were set at 2 kV and 40 V, respectively. For negative ion mode, the capillary and cone voltages were set at 1 kV and 40 V, respectively. Centroid mass spectrometry $(MS)^E$ mode was used to collect mass spectrometry data. The primary scan ranged from 50 to 1200 Da, and the scanning time was 0.2 seconds. All parent ions were fragmented using 20-40 eV. The information of all fragments was collected (using a time of 0.2 seconds). In the data acquisition process, the leucine enkephalin signal was gained every three seconds, for real-time quality correction. For accurate mass acquisition, leucine enkephalin (at a flow rate of 10 µL min^{-1}) was used as a lock mass by a lock spray interface to monitor the positive ($[M + H]^+$ = 556.2771) and negative ($[M - H]^-$ = 554.2615) ion modes. Data acquisition and analysis were controlled by Waters UNIFI V1.71 software. The scans in MS and MS/MS modes ranged between 50-1200 m/z (Figure 1).

Statistical Analysis

Results were analyzed using SPSS software, version 19.0 (SPSS, IBM, Armonk, NY, USA). To determine statistical differences in the inhibition of the B16 cells proliferation (after treatment with different concentrations of MEPT), we used a one-way analysis of variance (ANOVA) with the Tukey post-hoc tests across each MEPT treatment time point. Statistical significance was set at $p< 0.05$.

Results

MEPT Inhibits Melanoma Cell Growth

We examined the effect of MEPT on the growth of B16 cells by MTT assay. After treatment that lasted 24 hours, the highest growth inhibition in B16 cells (78.41 ± 0.82 %) occurred at 40 µM in a dose-dependent manner (Table I). After treatment with 40 µM MEPT for 48 hours, B16 cell growth inhibition rate was approximately 87.13 ± 0.49 % of the control rate value. After 72 hours of treatment, the B16 cell inhibition rate reached 97.34 ± 0.10% of the control rate with 40 µM, making this the most marked growth inhibition rate, and a significant decrease in the number of live cells was observed. As indicated in Figure 2A, the proliferation of B16 cells was significantly reduced, in a dose-dependent manner, when these cells were treated with MEPT over the course of three days ($p< 0.05$).

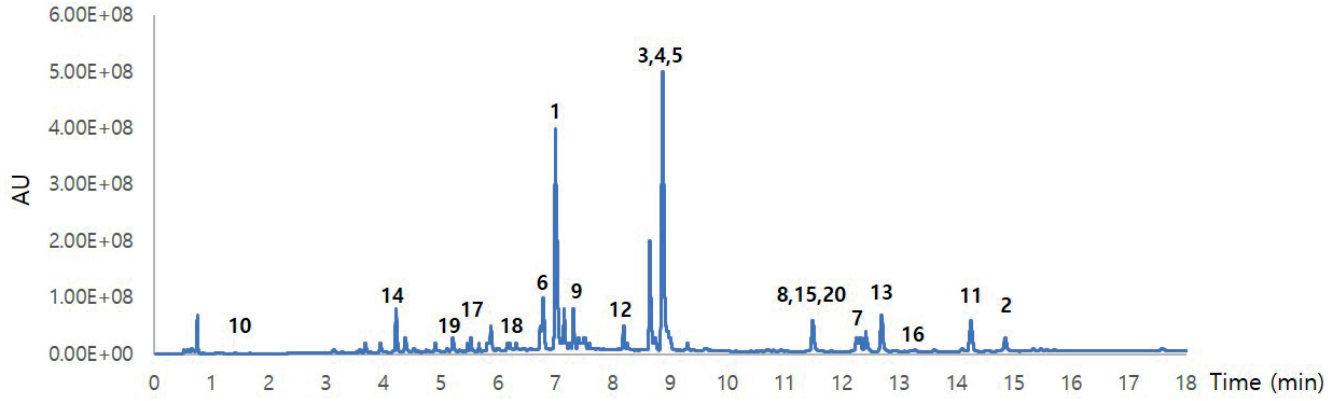

	Component name	Total Fragments Found	Formula	Mass error (mDa)	Observed RT (min)	Detector counts	Adducts
1	Quinofuracin A	45	C26H30O12	0.1	7.07	837288	+HCOO
2	25-hydroxyporicoic acid H	132	C31H48O6	-0.1	14.93	628808	+HCOO
3	Aeruginosin GE686	61	C29H44BrClN6O6	3	9.03	585741	-H
4	BK223 B	90	C42H48O20	2.5	9.03	555814	+HCOO
5	9-[(2R,5S)-5-(Hydroxymethyl)tetrahydro-2-furanyl]-3,9-dihydro-6H-purin-6-one - 4-[(E)-2-(3,5-dihydroxyphenyl)vinyl]phenyl beta-D-glucopyranosiduronic acid (1:1)	25	C30H32N4O12	-0.6	9.01	528449	-H
6	Quinofuracin A	38	C26H30O12	-0.5	6.85	403543	+HCOO
7	NGA0187	21	C30H48O6	0.4	12.6	324821	+HCOO, -H
8	Astellolide A	86	C26H30O8	0.5	11.88	289166	+HCOO, -H
9	Oxypaeoniflorin	17	C23H28O12	0.8	7.55	261145	+HCOO
10	Coaristeromycin	10	C11H14N4O4	-1.1	1.78	255669	-H
11	Milbemycin β10	36	C33H50O8	0	14.88	251680	+HCOO
12	Trioxacarcin E	47	C34H44O18	-0.3	8.21	242256	+HCOO, -H
13	Platycodigenin	104	C30H48O7	-0.5	12.73	220285	-H, +HCOO
14	Phomoeuphorbin A	14	C15H16O6	0	4.27	204135	+HCOO
15	2',3'-Epoxymyrothecine A	50	C27H34O10	0.3	11.48	192751	-H
16	Nomilin	35	C28H34O9	0.4	13.22	169919	+HCOO, -H
17	Paecilomycin J	49	C19H26O8	-0.2	5.72	163624	+HCOO
18	Talapolyester A	31	C22H30O12	-0.2	6.79	158768	-H
19	Phomoeuphorbin A	29	C15H16O6	-0.2	5.26	146882	+HCOO
20	NPA004109	34	C30H50O7	-0.7	11.68	144864	+HCOO

Figure 1. UPLC-MS and MS/MS chromatograms with data of immature fruit extract of *P. trifoliata*. Twenty peaks were discriminated and annotated according to their retention times. Each peak identified to one or several ions formed in the MS and MS/MS source, detected by the MS and MS/MS detector. UPLC, ultra-performance liquid chromatography; MS, mass spectrometry.

Table I. Inhibition rate of B16 cells after treatment with different concentrations of MEPT (n = 6).

	Concentration (μM)	24 h	48 h	72 h
MEPT	0	–*	–*	–*
	10	34.38 ± 1.23†	60.88 ± 0.734†	34.36 ± 1.32†
	20	46.01 ± 1.65‡	67.82 ± 0.98‡	51.66 ± 2.54‡
	30	57.47 ± 0.45¶	74.67 ± 0.27¶	74.06 ± 1.28¶
	40	78.41 ± 0.82^	87.13 ± 0.49^	97.34 ± 0.10^

Data are presented as mean ± SD %. Statistical significance was determined by one-way ANOVA in each group.

*, †, ‡, ¶, ^; Identical superscript letters indicate a non-significant difference between groups, based on Tukey's multiple comparison test.

MEPT, methanol extract of immature *P. trifoliata*; SD, standard deviation; ANOVA, analysis of variance.

MEPT Inhibits Invasiveness and Migration Properties of Melanoma Cells

Wound-healing and transwell assays were used to investigate cell invasiveness and migration, respectively. The invasive capacity of MEPT-treated B16 cells was dose-dependently decreased compared to that of control B16 cells ($p < 0.01$; Figure 2B). In addition, similar results were obtained in the transwell migration assay: melanoma cells treated with MEPT for 24 hours showed attenuated migratory properties compared to B16 cells in the control group ($p < 0.01$; Figure 2C).

Involvement of the PI3K-AKT Signalling Pathway in the Regulation of p21 by MEPT

Cell cycle analyses were performed to understand the mechanisms mediating the inhibitory effect of MEPT on melanoma cell growth, migration, and invasion. The results revealed that MEPT treatment significantly increased the percentage of cells in the G1 stage of the cell cycle ($p < 0.05$), suggesting that the cells were arrested in the G1 stage (Figure 3A). To verify these findings, we investigated whether MEPT influenced the proliferation of melanoma cells through the PI3K/AKT signalling pathway by determining the relative amounts of phosphorylated PI3K and AKT, as well as expression levels of cell cycle-related proteins, p21, and cyclin E. Western blotting of extracts from B16 cells treated with MEPT (for 24 hours) showed that MEPT dose-dependently and significantly decreased the levels of phosphorylated PI3K and AKT proteins (Figure 3B,C). In addition, no differences in total PI3K and AKT protein levels were found between the MEPT-treated and control B16 cells (Figure 3B). MEPT treatment downregulated cyclin E expression level, while p21 expression was significantly increased after MEPT treatment. Collectively, these data suggest that MEPT treatment might influence cell proliferation, migration, and invasiveness, *via* modulation of the PI3K/AKT signalling pathway.

MEPT Treatment Causes Mitochondrial Membrane Depolarisation in Melanoma Cells

Cell nuclei and mitochondria were stained using DAPI and MitoTracker Red CMXRos, respectively. MEPT treatment decreased mitochondrial membrane potential. As shown in Figure 4A, the percentage of dead cells significantly increased in B16 cells exposed to either 20 or 30 μM MEPT for 48 hours, compared to the percentage of dead cells in the control B16 cells.

We also used MitoTracker Red and DAPI to study the subcellular localisation of mitochondria and cell nuclei. B16 cells treated with MEPT for 48 hours showed dose-dependent changes in nuclear shape (DNA fragmentation), as well as an increase in the mitochondrial network (red intensity) in the cytoplasm (Figure 4B). In control cells, the mitochondrial membrane was intact, whereas B16 cells exposed to MEPT (10 and 20 μM) showed a dose-dependent loss of membrane integrity (Figure 4B). B16 cells treated with 30 μM MEPT displayed the highest number of ruptured mitochondria related to increased cell apoptosis.

MEPT Triggers Apoptosis Through Activation of the Mitochondrial Apoptosis Pathway

To examine the apoptotic cell death pathway induced by MEPT, we measured cytochrome c content in the cytosol and mitochondria of B16 cells treated with 0, 10, 20, and 30 μM MEPT, respectively, for 48 hours. As shown in Figure 4C, MEPT treatment dose-dependently increased and decreased cytochrome c levels in the cytosol and mitochondria, re-

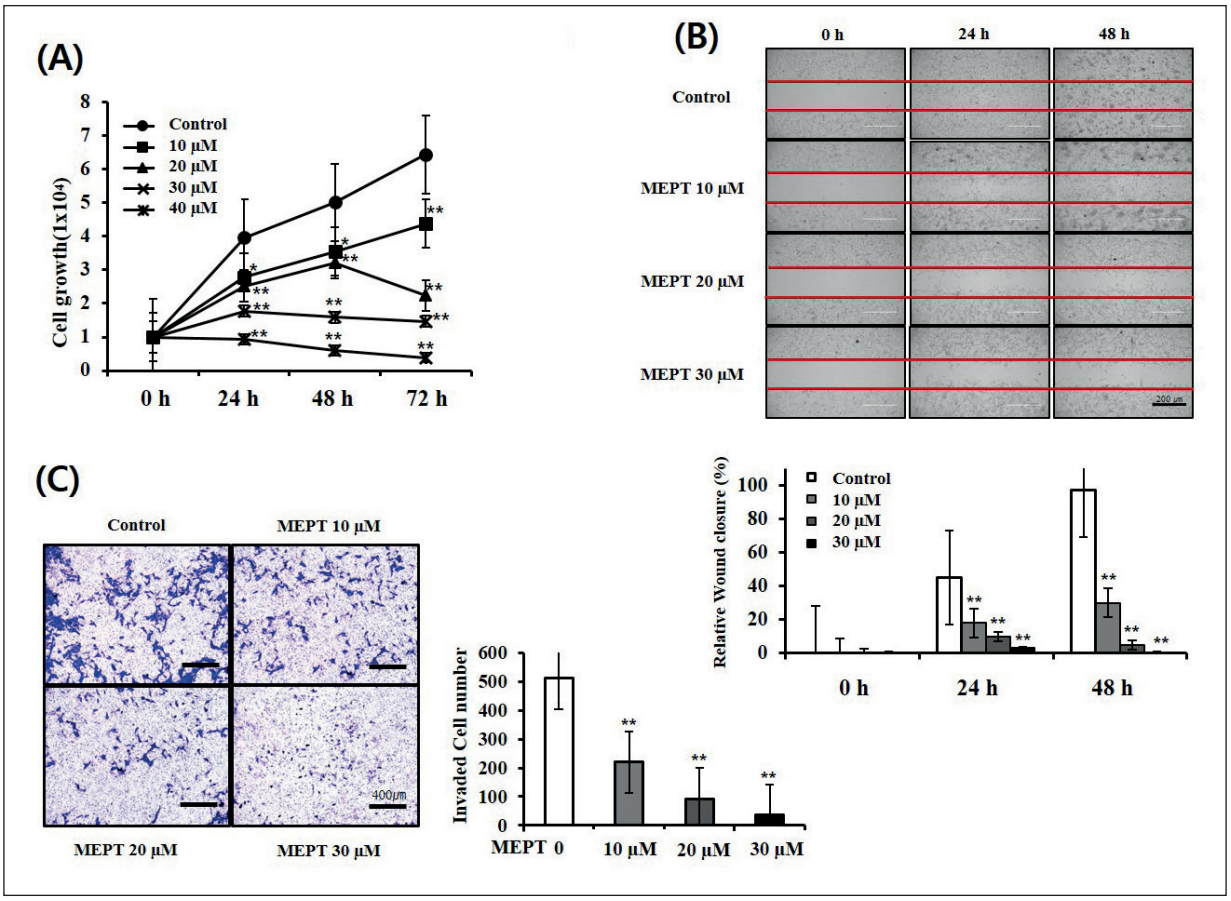

Figure 2. MEPT inhibits the survival, invasiveness, and migration of B16 cells. **A**, B16 cells were treated with 0, 10, 20, 30, or 40 μM MEPT for either 0, 24, 48, and 72 hours, respectively. The proportion of surviving/proliferating cells was analysed using the MTT assay. MEPT inhibited cell growth in a concentration-dependent manner. **B**, Cell invasiveness, assessed using the wound scratch test (magnification: 100×), was measured in the presence of 0, 10, 20, or 30 μM MEPT for 0, 24, and 48 hours. The upper part of the panel shows images of the representative experiments. The graph in the lower part of the panel illustrates the extent of relative wound closure. **C**, Transwell migration assay showed that, in the presence of MEPT, the number of migrated B16 cells was lower than in the control group. The scale bar corresponds to 400 μm. The right panel illustrates the relationship between the number of migrated cells and MEPT concentration. The graph is representative of three independent experiments. Data are presented as the mean ± standard error of the mean. Statistical significance of differences from control B16 cells is indicated as follows: *p<0.05, **p<0.01 *vs.* untreated cells. MEPT, methanol extract of immature *P. trifoliata*; MTT, 3- (4,5-dimethylthiazol-2-yl)-2,5-diphenyltetrazolium bromide

spectively. The release of cytochrome c, which was evident after treatment with 20 μM MEPT, suggested might be important in MEPT-induced apoptosis.

To further clarify the basic mechanism of MEPT-induced mitochondrial apoptosis, we studied Bcl-2 (an anti-apoptotic protein) expression levels and Bax and Apaf-1 (pro-apoptotic proteins) expression levels in B16 cells after they were exposed to 48 hours of MEPT treatment. As shown in Figure 4C, exposing B16 cells to MEPT significantly increased the relative expression levels of Apaf-1 and Bax in a dose-dependent manner, whereas Bcl-2 expression significantly decreased after MEPT exposure.

Since cell cycle data indicated that a significant proportion of MEPT-treated cells were in the G1 (apoptotic) phase, we used Hoechst 33342 nuclear staining to perform a qualitative assessment of apoptosis. As shown in Figure 5A, cell treatment with high concentrations of MEPT led to nuclear condensation and fragmentation – a feature that was not observed in control B16 cells.

To confirm our observation that MEPT indeed induced apoptosis, MEPT-treated B16 cells were stained with Annexin V-FITC/PI and analyzed using flow cytometry. These experiments confirmed the dose-dependent effect of MEPT on B16 cell apoptosis (Figure 5B; $p < 0.01$). In addition, total

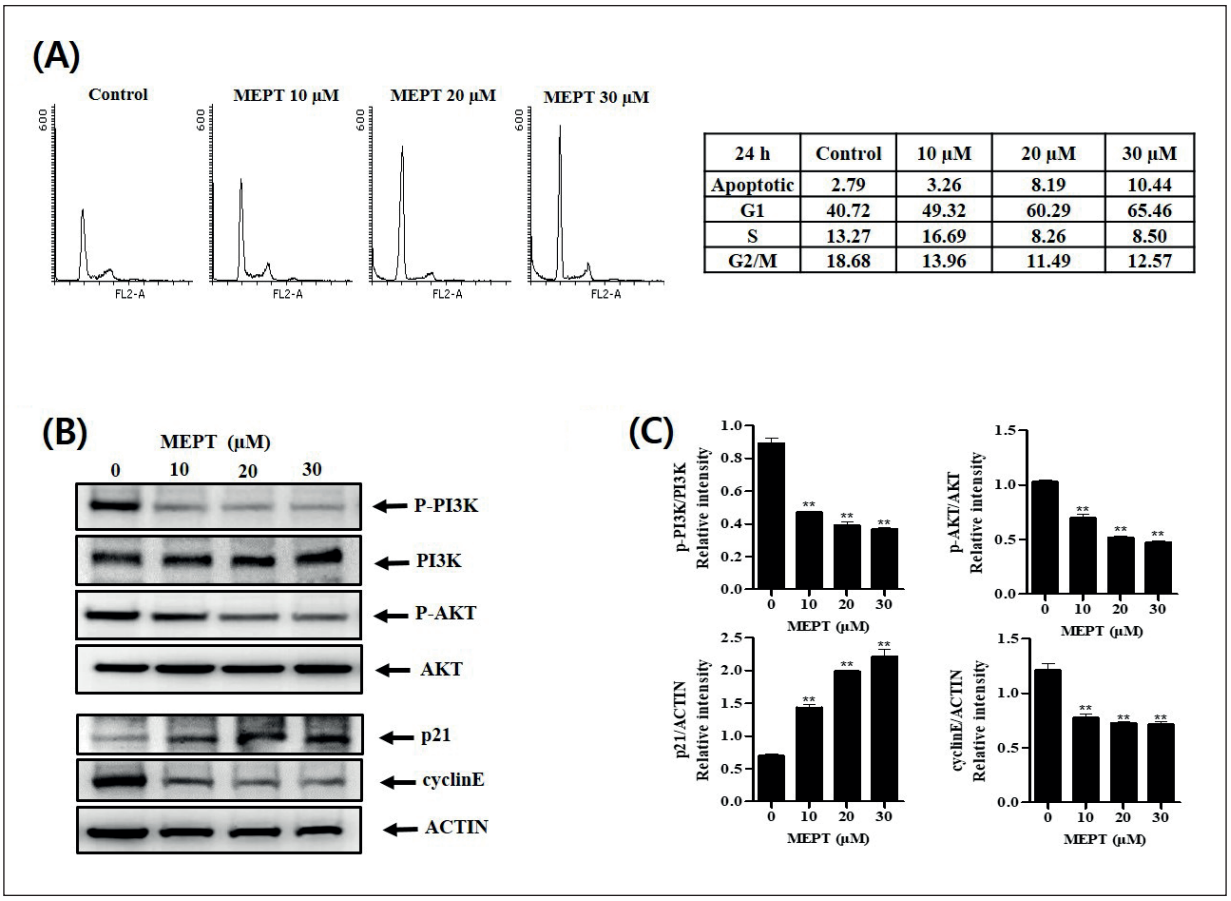

24 h	Control	10 μM	20 μM	30 μM
Apoptotic	2.79	3.26	8.19	10.44
G1	40.72	49.32	60.29	65.46
S	13.27	16.69	8.26	8.50
G2/M	18.68	13.96	11.49	12.57

Figure 3. Cell cycle arrest and changes in the levels of cell cycle-related proteins (PI3K/AKT/p21 signaling pathway) in MEPT-treated B16 cells. **A**, Cell cycle distributions of B16 cells, measured using flow cytometry, at 24 hours after treatment with 10, 20, or 30 μM MEPT, respectively, were analyzed and compared to those of control B16 cells. **B**, In MEPT-treated cells, levels of p-PI3K, PI3K, p-AKT, AKT, p21, and cyclin E were examined using western blotting. Cells were treated with MEPT, at different concentrations, for 24 hours. **C**, Quantitative analyses of the levels of p-PI3K, PI3K, p-AKT, AKT, p21, and cyclin E in MEPT-treated B16 cells. Actin was used as loading control. The graph is representative of three independent experiments. Data are presented as the mean ± standard error of the mean. Statistical significance of differences from control B16 cells is indicated as follows: $^{**}p < 0.01$. *vs.* untreated cells. MEPT, methanol extract of immature *P. trifoliata*; PI3K, phosphoinositide-3-kinase ; AKT, protein kinase B

cell lysates were analyzed to detect the expression of cleaved caspase-9, caspase-3, and PARP, using western blotting. As shown in Figure 5C, cleaved caspase-9, caspase-3, and PARP levels were significantly increased in MEPT-treated B16 cells, in a dose-dependent manner. The mitochondrial apoptosis pathway in B16 cells was thus activated as a result of MEPT treatment.

Discussion

P. trifoliata fruits of different degrees of maturity possess distinct pharmacological qualities, affecting gastrointestinal motility and exhibiting both anti-inflammatory and anticancer effects[9]. Given the pharmacological characterization of the biologically active constituents of this plant, this study aimed to examine the effectiveness of the immature *P. trifoliata* fruit extract on melanoma cells and assess the use of immature *P. trifoliata* fruit extract in melanoma treatment.

Malignant melanoma is characterized by the propensity for metastases, drug resistance, and high mortality[11]. Due to the lack of effective treatment for malignant melanoma, novel candidate therapeutics are urgently needed. Common chemotherapy generally remains the treatment of choice for the most invasive malignancies, but problems pertaining to chemotherapy (such as serious side effects and rapid development of drug resistance) are still prevalent, despite its use.

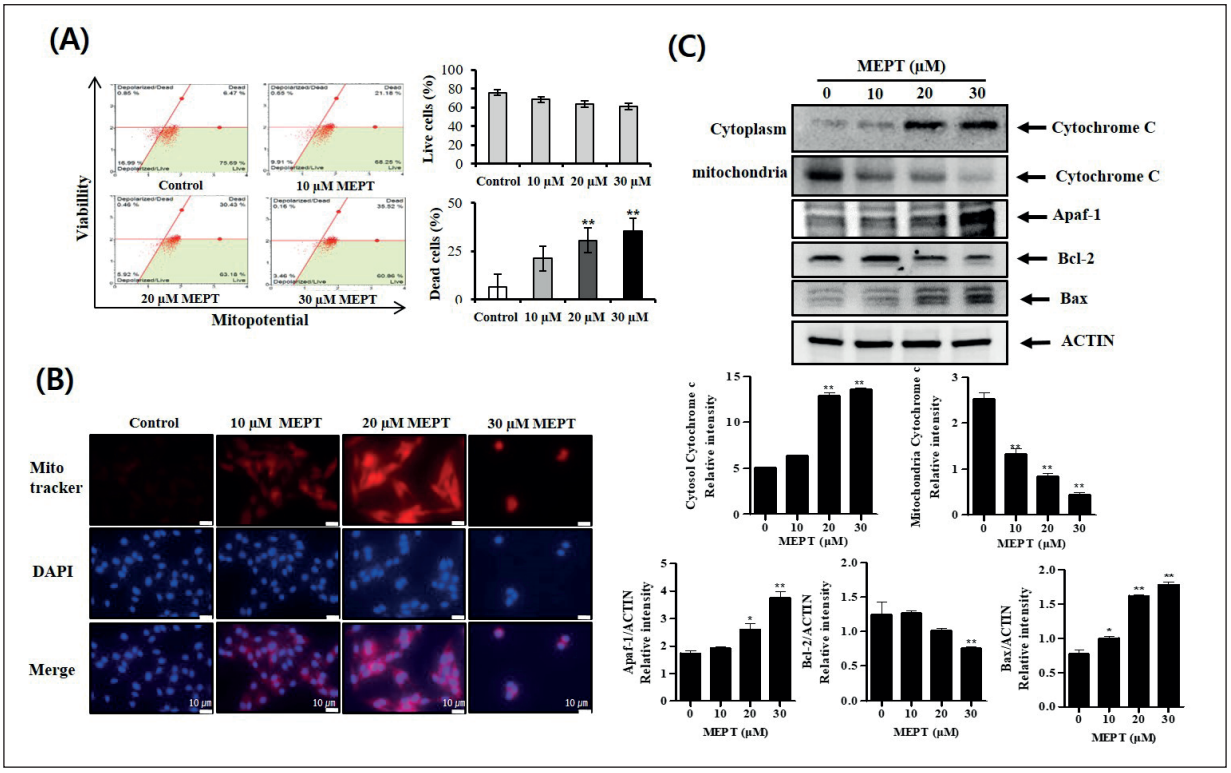

Figure 4. MEPT-induced cell apoptosis *via* the mitochondrial signaling pathway. **A**, The influence of MEPT, at different concentrations, on mitochondrial membrane potential in B16 cell cultures, following 48-hour incubation. The analysis was performed by using the Muse® MitoPotential Assay Kit. Typical scatter plots showing the percentages of live and dead depolarized cells are indicated for one experiment. The graphs represent the mean percentages of live and dead cells for three independent experiments. **B**, Representative MitoTracker Red CMXRos and DAPI staining (blue) of B16 cells, through an inverted microscope (Olympus H4-100, CCD camera) and a 40× objective. Scale bar, 10 μm. **C**, Western blotting analysis of changes in the relative levels of cytochrome c, Apaf-1, Bcl-2, and Bax after treatment with MEPT, at different concentrations, for 24 hours. The upper part of the panel shows the representative blots. Quantitative analysis of western blotting data is illustrated in the graphs in the lower part of the panel. Actin signal was used as loading control. Each graph is representative of three independent experiments. Data are presented as the mean ± standard error of the mean. Statistical significance of differences from the levels in control B16 cells is indicated as follows: $*p< 0.05$, $**p< 0.01$ *vs.* untreated cells. MEPT, methanol extract of immature *P. trifoliata*.; DAPI, 4′,6-diamidino-2-phenylindole

Therefore, the search for more therapeutic and less toxic anticancer drugs is warranted. *P. trifoliata* may be a source of natural compounds that potentially act as anticancer agents.

Several studies[12-15] have recently shown that the chemical constituents of mature *P. trifoliata* fruit extracts display anticancer effects, but the antitumor activity of immature *P. trifoliata* fruit extracts has not been properly elucidated. Mature fruit extracts can effectively inhibit the proliferation of several types of cancer cells by causing G1 phase cell cycle arrest (inducing apoptosis) or by stimulating antioxidant activity (exerting anticancer effects)[9]. The current study is the first to report the effects of immature *P. trifoliata* extract on melanoma cells *in vitro*. We observed that MEPT attenuated cell cycle progression, inhibited migration capacity, and caused apoptosis in B16 melanoma cells. Among the mechanisms underlying these effects, changes in mitochondrial membrane potential and in the levels of pro-apoptotic markers (such as caspases 3/9/PARP) were present.

First, we found that treating B16 cells with MEPT led to a significant and dose-dependent decrease in both their viability and propensity for migration and invasion. Secondly, based on cell cycle analyses, we found that MEPT led to a significant number of cells being arrested in the G1 phase of the cell cycle, depending on the extract concentration. Growth arrest in the G1 phase prompted B16 cells to undergo apoptosis, which was confirmed based on the observations of characteristic apoptotic changes in cell morphology. Inhibiting the progression of deregulated cell

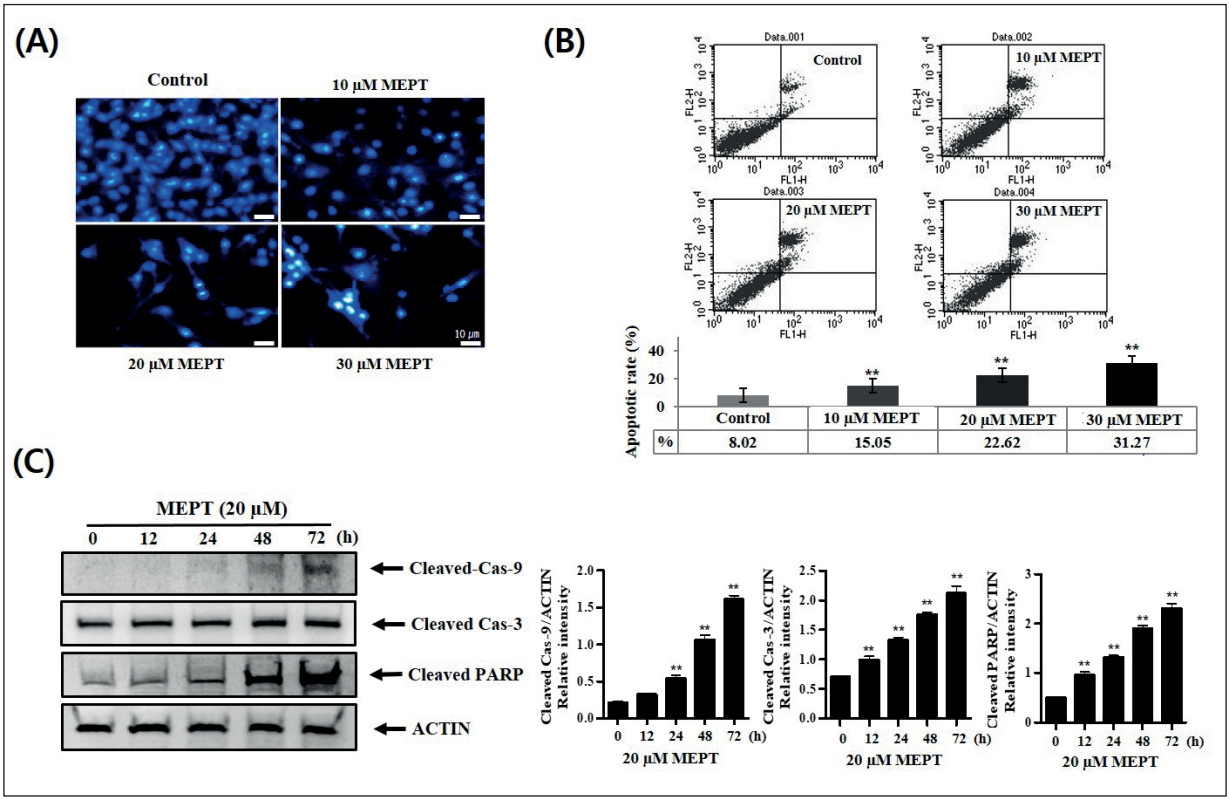

Figure 5. MEPT induces apoptosis in B16 cells. **A**, B16 cells were incubated with MEPT (at different concentrations), stained with Hoechst 33342 (to assess the extent of cellular apoptosis), and examined under a fluorescent microscope (magnification: 40×). The scale bar corresponds to 10 μm. **B**, B16 cells were stained with annexin V and analysed by flow cytometry. Quantitative analysis of the fraction of apoptotic B16 cells in control conditions, following incubation with MEPT at different concentrations. **C**, Western blotting analysis of changes in the relative levels of cleaved caspase-9, cleaved caspase-3, and cleaved PARP expression in B16 cells treated 20 μM MEPT, for various time periods. The left part of the panel shows representative blots. Quantitative analysis of western blotting data is illustrated in the graphs in the right part of the panel. Actin was used as a loading control. Data are presented as the mean ± standard error of the mean. Statistical significance of differences from the levels in control B16 cells is indicated as follows: $^{**}p < 0.01$. MEPT, methanol extract of immature *P. trifoliata*; PARP, poly (adenosine diphosphate-ribose) polymerase.

cycles in tumor cells is an effective stratagem to stop the growth of cancer cells[16]. Therefore, morphological observations and cell cycle arrest indicated that MEPT hindered the survival of melanoma cells by prompting apoptosis *in vitro*. Thirdly, our study indicated that MEPT induced apoptosis of melanoma cells *via* mitochondrial pathways. MEPT has already been proven to cause apoptosis in colorectal carcinoma, hepatoma, and oral squamous cell carcinoma cells[10,17,18].

Melanoma is a heterogeneous tumor. Depending on an individual's race, as well as the pathogenic location and histological type of the tumor, melanomas may be triggered by mutations and amplification of a diverse set of genes that cause abnormal signaling in mitogen-activated protein kinase, KIT, PI3K-AKT, and other pathways[11]. The PI3K/AKT signaling pathway is one of the main pathways involved in the activation of the cell cycle regulatory protein, p21[19]. Therefore, we further investigated the effects of MEPT on the proteins in this pathway. Our findings indicated that inhibition of the PI3K-AKT signaling pathway was involved in MEPT-induced increased p21 expression. The role of PI3K/AKT pathway signaling in cell cycle progression, apoptosis prevention, and malignant transformation is well documented[20]. Cell cycle progression is controlled by a series of signaling cascades that regulate DNA replication, allowing for cell division and growth. Cyclin E binds to cyclin-dependent kinase 2 in the G1 phase, initiating DNA duplication and the transition from the G1 to S phase of the cell cycle[21]. Our experiments showed that p21 and cyclin E expression were dose-dependently elevated 24 hours after the start of MEPT treatment.

Apoptosis is accompanied by both upregulation and downregulation of either pro-apoptotic or anti-apoptotic proteins, respectively. The pro-apoptotic protein, Bax, and the anti-apoptotic protein, Bcl-2, are key role players in apoptosis[22]. In this study, changes in the levels of both Bax and Bcl-2 likely played a role in MEPT-induced apoptosis of melanoma cells. Bax activation and Bcl-2 inhibition lead to a loss in mitochondrial membrane potential and an increase in mitochondrial membrane permeability[23,24]. As a result, cytochrome c and apoptosis-inducing factors are released from the mitochondria to the cytosol. Through this mechanism, mitochondria play an important part in apoptosis regulation[25]. Chemotherapy-induced apoptosis stimulates the release of apoptotic factors, such as cytochrome c, from mitochondria to the cytosol[26]. Subsequently, cytosolic cytochrome c forms an apoptosome complex with Apaf-1 and adenosine triphosphate, activating procaspase-9, eventually leading to caspase-3 activation. Caspase-3 is a major mediator of apoptosis[27]. Mitochondrial dysfunction includes the altered release of the intermembrane space protein, cytochrome c. Released cytochrome c activates Apaf-1, which commences a caspase-activation pathway. Activated caspases can also affect mitochondrial action[28]. Caspases can be activated indirectly (through Apaf-1-cytochrome c interactions) or directly, following activation of death receptors on cell surfaces and caspases themselves (for example, caspase-3), where caspases are activated through double cleavage[22]. The cleaved caspase, which consists of two large and two small subunits, activates death substrates (such as PARP) to ultimately cause cell death[27]. In this study, the treatment of B16 cells with MEPT significantly reduced mitochondrial membrane potential and increased cytosolic levels of cytochrome c, Apaf-1, cleaved caspase-9, cleaved caspase-3, and cleaved PARP. This study was limited only to *in vitro* experimentation. Moreover, the effects of both immature and mature *P. trifoliata* fruit extracts on melanoma B16 cells were not compared. Despite these limitations, our results indicated that MEPT treatment induced apoptosis of B16 cells by inhibiting the PI3K/AKT mitochondrial pathway.

Conclusions

Collectively, our experiments demonstrated that the anticancer effect of MEPT was mediated by the induction of apoptosis. To the best of our knowledge, our study is the first to show the anticancer effect of MEPT in B16 melanoma cells. Based on previous reports by our study group and other researchers, we could reasonably conclude that MEPT triggered apoptosis of melanoma cells through the activation of mitochondrial apoptosis pathways, loss of mitochondrial membrane potential, and increased activity of caspase pathways. Therefore, MEPT may contain bioactive phytochemicals for the chemoprevention or chemotherapy of melanoma. However, MEPT is only a partially purified complex of glabretal triterpenes – not a pure compound. Therefore, it will be necessary to identify the components of MEPT that are specifically responsible for the induction of apoptosis. Regardless, our present results allow for a preliminary conclusion that MEPT constitutes a valuable source of natural compounds that are useful in the treatment of melanoma.

Conflicts of Interest

The authors declare that they have no conflict of interest.

Institutional Review Board Statement

Not applicable.

Authors' Contributions

S.K. and M.K. conceived the idea of the experiment. S.K., H.Y., B.Y., and H.P. carried out the experiments. I.H., M.J., M.K., and I.C. analyzed the data. S.K. and M.K. wrote the manuscript. All authors read and agreed with the final submitted version.

Funding

This work was supported by the Fund of the Biomedical Research Institute of the Jeonbuk National University Hospital.

ORCID ID

Sun-Young Kim: 0000-0001-7898-0801
Iee Ho Choi: 0000-0003-0935-7463
Min Jung Han: 0000-0002-9311-5370
Ho-Keun Yi: 0000-0003-4403-3827
Bong-Sik Yun: 0000-0002-0594-8955
Hae-Ryong Park: 0000-0003-2168-7393
Minsun Kim: 0000-0002-3617-7823

Data Availability Statement

The datasets generated and/or analyzed during the current study are available from the corresponding author on reasonable request.

References

1) Domingues B, Lopes JM, Soares P, Pópulo H. Melanoma treatment in review. Immunotarg ets Ther 2018; 7: 35-49.
2) Miller AJ, Mihm MCJ. Melanoma. N Engl J Med 2006; 355: 51-65.
3) American Cancer Society, "Cancer Facts & Figures." Available from: http://www.cancer.org/acs/groups/content/@editorial/documents/document/acspc-048738.pdf, 2017 [Accessed November 2017].
4) Ferlay J, Soerjomataram I, Dikshit R, Eser S, Mathers C, Rebelo M, Parkin DM, Forman D, Bray F. Cancer incidence and mortality worldwide: sources, methods and major patterns in GLOBOCAN 2012. Int J Cancer 2015; 136: E359-E386.
5) Jiang BP, Zhang L, Guo XL, Shen X, Wang Y, Zhu Y, Liang H. Poly (N-phenylglycine)-based nanoparticles as highly effective and targeted near-infrared photothermal therapy/photodynamic therapeutic agents for malignant melanoma. Small 2017; 13: Article ID 1602496.
6) Bombelli FB, Webster CA, Moncrieff M, Sherwood V. The scope of nanoparticle therapies for future metastatic melanoma treatment. Lancet Oncol 2014; 15: e22-e32.
7) Balch CM, Gershenwald JE, Soong SJ, Thompson JF, Atkins MB, Byrd DR, Buzaid AC, Cochran AJ, Coit DG, Ding S, Eggermont AM, Flaherty KT, Gimotty PA, Kirkwood JM, McMasters KM, Mihm JMC, Morton DL, Ross MI, Sober AJ, Sondak VK. Final version of 2009 AJCC melanoma staging and classification. J Clin Oncol 2009; 27: 6199-6206.
8) Kim BY, Yoon HY, Yun SI, Woo ER, Song NK, Kim HG, Jeong SY, Chung YS. In vitro and in vivo inhibition of glucocorticoid-induced osteoporosis by the hexane extract of Poncirus trifoliata. Phytother Res 2011; 25: 1000-1010.
9) Jang Y, Kim EK, Shim WS. Phytotherapeutic effects of the fruits of Poncirus trifoliata (L.) Raf. on cancer, inflammation, and digestive dysfunction. Phytother Res 2018; 32: 616-624.
10) Kim SY, Yi HK, Yun BS, Lee D, Hwang PH, Park HR, Kim M. The extract of the immature fruit of Poncirus trifoliata induces apoptosis in colorectal cancer cells via mitochondrial autophagy. Food Sci Hum Wellness 2020; 9: 237-244.
11) Luo C, Shen J. Research progress in advanced melanoma. Cancer Lett 2017; 397: 120-126.
12) Han HY, Ryu MH, Son Y, Lee G, Jeong SH, Kim H. Poncirus trifoliata Rafin. induces the apoptosis of triple-negative breast cancer cells via activation of the c-Jun NH (2)-terminal kinase and extracellular signal-regulated kinase pathways. Pharmacogn Mag 2015; 11: 237-243.
13) Xu F, Zang J, Chen D, Zhang T, Zhan H, Lu M, Zhuge H. Neohesperidin induces cellular apoptosis in human breast adenocarcinoma MDA-MB-231 cells via activating the Bcl-2/Bax-mediated signaling pathway. Nat Prod Commun 2012; 7: 1475-1478.
14) Hong J, Min HY, Xu GH, Lee J, Lee S, Kim YS, Kang SS, Lee SK. Growth inhibition and G1 cell cycle arrest mediated by 25-methoxyhispidol A, a novel triterpenoid, isolated from the fruit of Poncirus trifoliata in human hepatocellular carcinoma cells. Planta Med 2008; 74: 151-155.
15) Rahman A, Siddiqui SA, Jakhar R, Kang SC. Growth inhibition of various human cancer cell lines by imperatorin and limonin from Poncirus trifoliata Rafin. Seeds. Anticancer Agents Med Chem 2015; 15: 236-241.
16) Singh RP, Dhanalakshmi S, Agarwal R. Phytochemicals as cell cycle modulators--a less toxic approach in halting human cancers. Cell Cycle 2002; 1: 156-161.
17) Han H, Park BS, Lee GS, Jeong S, Kim H, Ryu JH. Autophagic cell death by Poncirus trifoliata Rafin., a traditional oriental medicine, in human oral cancer HSC-4 cells. Evid Based Complement Alternat Med 2015; 2015: Article ID 394263.
18) Pokharel YR, Han EH, Kim JY, Oh SJ, Kim SK, Woo E, Jeong HG, Kang KW. Potent protective effect of isoimperatorin against aflatoxin B1-inducible cytotoxicity in H4IIE cells: Bifunctional effects on glutathione S-transferase and CYP1A. Carcinogenesis 2006; 27: 2483-2490.
19) Hu Z, Long T, Ma Y, Zhu J, Gao L, Zhong Y, Wang X, Wang X, Li Z. Downregulation of GLYR1 contributes to microsatellite instability colorectal cancer by targeting p21 via the p38MAPK and PI3K/AKT pathways. J Exp Clin Cancer Res 2020; 39: 76.
20) Chang F, Lee JT, Navolanic PM, Steelman LS, Shelton JG, Blalock WL, Franklin RA, McCubrey JA. Involvement of PI3K/AKT pathway in cell cycle progression, apoptosis, and neoplastic transformation: A target for cancer chemotherapy. Leukemia 2003; 17: 590-603.
21) Hinds PW, Mittnacht S, Dulic V, Arnold A, Reed SI, Weinberg RA. Regulation of retinoblastoma protein functions by ectopic expression of human cyclins. Cell 1992; 70: 993-1006.
22) Gross A, McDonnell JM, Korsmeyer SJ. BCL-2 family members and the mitochondria in apoptosis. Genes Dev 1999; 13: 1899-1911.
23) Roy AM, Baliga MS, Elmets CA, Katiyar SK. Grape seed proanthocyanidins induce apoptosis through p53, Bax, and caspase 3 pathways. Neoplasia (New York, N.Y.) 2005; 7: 24-36.
24) Chipuk JE, Kuwana T, Bouchier-Hayes L, Droin NM, Newmeyer DD, Schuler M, Green DR. Direct activation of Bax by p53 mediates mitochondrial membrane permeabilization and apoptosis. Science 2004; 303: 1010-1014.
25) Tong X, Lin S, Fujii M, Hou DX. Echinocystic acid induces apoptosis in HL-60 cells through

mitochondria-mediated death pathway. Cancer Lett 2004; 212: 21-32.

26) Kim R, Tanabe K, Uchida Y, Emi M, Inoue H, Toge T. Current status of the molecular mechanisms of anticancer drug-induced apoptosis. The contribution of molecular-level analysis to cancer. Chemotherapy. Cancer Chemother Pharmacol 2002; 50: 343-352.

27) Chen Q, Liu XF, Zheng PS. Grape seed proanthocyanidins (GSPs) inhibit the growth of cervical cancer by inducing apoptosis mediated by the mitochondrial pathway. PloS One 2014; 9: e107045.

28) Garrido C, Galluzzi L, Brunet M, Puig PE, Didelot C, Kroemer G. Mechanisms of cytochrome c release from mitochondria. Cell Death Differ 2006; 13: 1423-1433.